# Experimental Verification of Characteristic Mode Analysis (CMA) using Reverberation Chamber

Haran Manoharan[#1], Xu Wang[#2], Matthew Wu[*3], Jagan Rajagopalan[*4], Akshay Mohan[*5] and Chulsoon Hwang[#6]

[#]*EMC Laboratory, Missouri University of Science and Technology*, Rolla, Mo, USA
[*]*Amazon Lab126, Sunnyvale, CA, USA*
[1]hm6h6, [2]xw7dh, [6]hwangc@mst.edu, [3]menghsi@amazon.com, [4]rrajagop, [5]aksmohan@lab126.com

2023 Joint Asia-Pacific International Symposium on Electromagnetic Compatibility and International Conference on ElectroMagnetic Interference & Compatibility (APEMC/INCEMIC) | 979-8-3503-3834-8/23/$31.00 ©2023 IEEE | DOI: 10.1109/APEMC57782.2023.10217353

***Abstract*—In this work, a novel experimental validation of characteristic mode analysis (CMA) is proposed using reverberation chamber measurements. Using the modal weighting coefficient formulation based on the magnetic moment and modal H field obtained from solvers, the total radiated power (TRP) is calculated. This TRP is compared with the TRP obtained from the reverberation chamber measurements. A good correlation between the simulation and measurement was achieved for a simple rectangular plate of size 15 cm × 8 cm with an error of less than 4 dB.**

***Keywords—characteristic mode analysis; CMA; reverberation chamber; total radiated power; modal weighting coefficients***

## I. Introduction

Characteristic mode analysis (CMA) is widely used to characterize the modal resonant behavior of arbitrarily shaped objects. It decomposes the currents induced on the conducting body in a set of fundamental modes [1]. CMA has been widely used in antenna analysis and design [2]-[4]. Recently, CMA received attention in the electromagnetic compatibility (EMC) community and has been applied to electromagnetic interference (EMI) [5][6] and radio frequency interference [7].

Experimental validations of CMA are important and essential, especially for EMC applications where complicated systems are analyzed. In [8], CMA was employed to find the excitation position to excite the required modes from the rectangular box, and radiation efficiency from simulation and measurement was correlated. The authors in [5] proposed using CMA to identify the radiation hotspots from a PCB excited by a cable. The total radiated power (TRP) from simulation and measurement was correlated. In all the previous works, the TRP from the device under test (DUT) with specific excitation in both simulation and measurement was studied. However, there is little work done to validate the CMA framework without a specific excitation.

In this paper, a new measurement setup is proposed to validate an excitation-free CMA analysis. The setup incorporates an H-field scanning system and reverberation chamber and can measure the modal weighting coefficient (MWC) based on magnetic moment excitation, which is the contribution of each location to the TRP. The TRP analytically calculated using the magnetic moment based MWC showed a good correlation with the measurement results.

This work was supported in part by the National Science Foundation (NSF) under Grant No. IIP-1916535.

## II. Theory of Characteristic Modes

For the completeness of the paper, the basic theory of CMA is briefly reiterated here, and detailed explanations are given in [9]. The generalized eigenvalue equation with $J_n$ and $\lambda_n$ representing eigenvectors and eigenvalues, respectively, is given by (1)

$$XJ_n = \lambda_n RJ_n \tag{1}$$

Modal significance (MS) is independent of the excitation and intrinsic property of the modes. It states the coupling capability of each mode with external sources. The modal significance is given by (2). The modes with modal significance 1 are called resonant modes, and this MS has a value range of [0,1].

$$MS = \left|\frac{1}{1+j\lambda_n}\right| \tag{2}$$

The MWC gives the coupling of the external excitation to the characteristic currents. This is not an intrinsic property and depends on the position and other factors of the external source. The MWC ($a_n$) is given as

$$a_n = \frac{\langle E^i_{\tan}(r), J_n\rangle}{1+j\lambda_n} \tag{3}$$

Since $a_n$ depends on the integral over the surface of the conducting body, separate simulations are required for each location of the source, which is a time-consuming process [7]. In [9], instead of using the delta gap voltage source and plane wave source cases, Harrington formulated MWC based on infinitesimal magnetic dipole sources.

$$a_n = -\frac{M \bullet H_n(r_o)}{1+j\lambda_n} \tag{4}$$

Here $H_n(r_o)$ is the modal H field at the location of the dipole source $r_o$, and M is the magnetic moment. To obtain the distribution of MWC over the entire area of the DUT for a given source, CMA simulations must be run for each location of the source over the DUT. This process can be time-consuming and resource intensive. However, using the formulation in (4) allows for only one CMA simulation of the DUT alone to be required. By scanning the plane over the structure of the DUT and using the simulation results of the modal H field and eigenvalue, MWC at any specific location of the source over the DUT can be calculated easily, which saves time and resources.

Based on the complex pointing theorem, the radiated power of each mode is the square of the absolute value of the MWC [5], as shown in (5). The total radiated power is the summation of the radiated power of all modes, as shown in (6).

$$P_n^{rad} = |a_n|^2 \tag{5}$$

$$TRP = \sum_n P_n^{rad} \tag{6}$$

## III. Proposed Measurement Setup

The reverberation chamber was used to measure the TRP. An H-field scanning system is used to capture the spread of MWC over the entire area of DUT. The H field probe was connected to port 1 of the vector network analyzer (VNA), and a biconical antenna was connected to port 2 of the VNA. The idea is to excite the structure using the H field probe, and total radiated power is obtained. The H field probe is placed around 2 mm above the DUT. The movement of the H field probe over the DUT is controlled by a stepper motor. The diagram of the experimental setup is shown in Fig.1. Fig. 2 shows the actual setup inside the reverberation chamber.

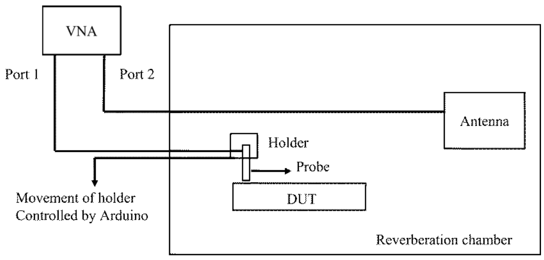


Fig. 1 Diagram of the measurement setup.

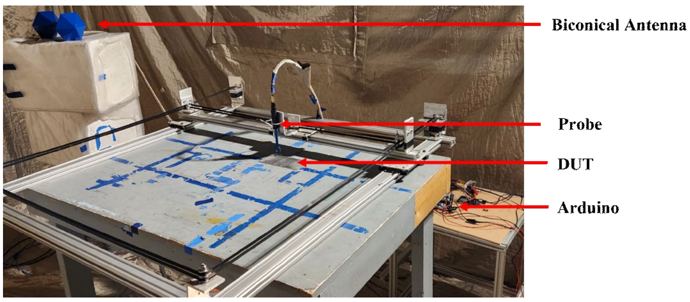


Fig. 2 Measurement setup inside the reverberation chamber.

The TRP from the DUT alone is obtained by (7), where $S_{21}^{DUT}$ is averaged magnitude of S21 between the probe (with DUT) and antenna, $S_{21}^{Ref}$ is averaged magnitude of S21 between the probe (without DUT) and antenna [5].

$$TRP = \left( \frac{\left(\langle |S_{21}^{DUT}| \rangle\right)^2}{\left(\langle |S_{21}^{Ref}| \rangle\right)^2} \right) \tag{7}$$

## IV. Validation

The DUT considered for validation is a rectangular plate of size 15 cm × 8 cm. The DUT is shown in Fig. 3. The CMA is carried out in CST MWS. The frequency range is set from 500 MHz to 1 GHz.

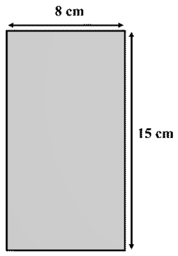


Fig. 3 Model of the rectangular plate.

### A. Simulation Results

Tables I and II give the modal significance and eigenvalues of the first five modes at four frequency points (500 MHz, 600 MHz, 800 MHz, and 1 GHz), respectively.

TABLE I. Modal Significance

| Mode # | Modal Significance | | | |
|---|---|---|---|---|
| | 500 MHz | 600 MHz | 800 MHz | 1 GHz |
| 1 | 0.205 | 0.419 | 0.958 | 0.977 |
| 2 | 0.056 | 0.096 | 0.223 | 0.401 |
| 3 | 0.0023 | 0.005 | 0.026 | 0.087 |
| 4 | 0.0018 | 0.004 | 0.019 | 0.061 |

TABLE II. Eigenvalue

| Mode # | Eigenvalue | | | |
|---|---|---|---|---|
| | 500 MHz | 600 MHz | 800 MHz | 1 GHz |
| 1 | -4.75 | -2.16 | -0.29 | 0.213 |
| 2 | -17.74 | -10.29 | -4.36 | -2.283 |
| 3 | -420.76 | -167.53 | -37.63 | -11.43 |
| 4 | -542.20 | -219.39 | -51.28 | -16.34 |

The modal H fields for the five modes are obtained from the solver, and based on (4), the MWC for each mode is calculated, and they are summed up to get the TRP.

### B. Measurement Results

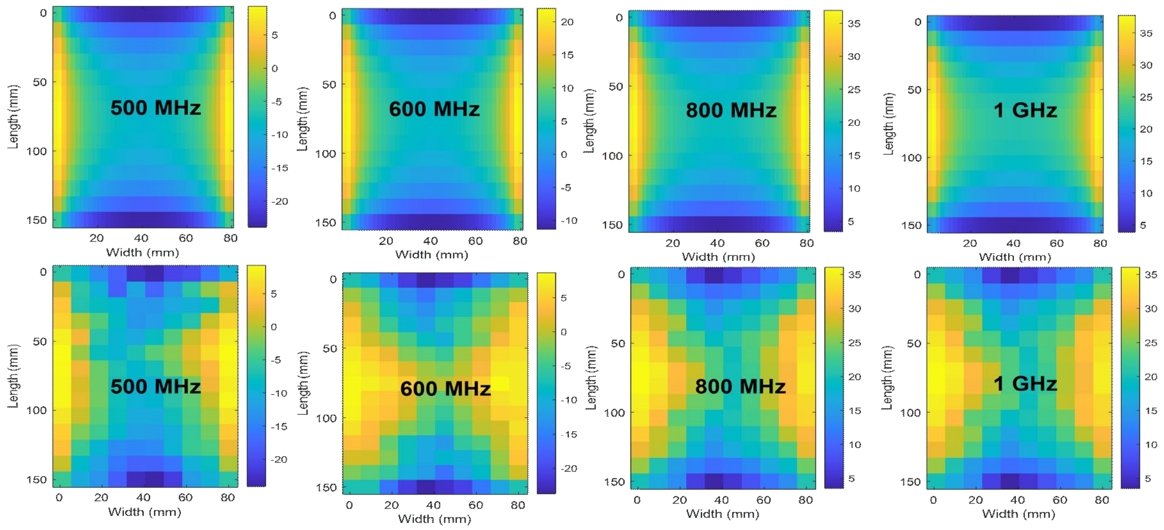


Fig. 4 Comparison of Simulated (1st row) vs. Measured (2nd row) $H_x$ $\sum |a_n|^2$ (dB).

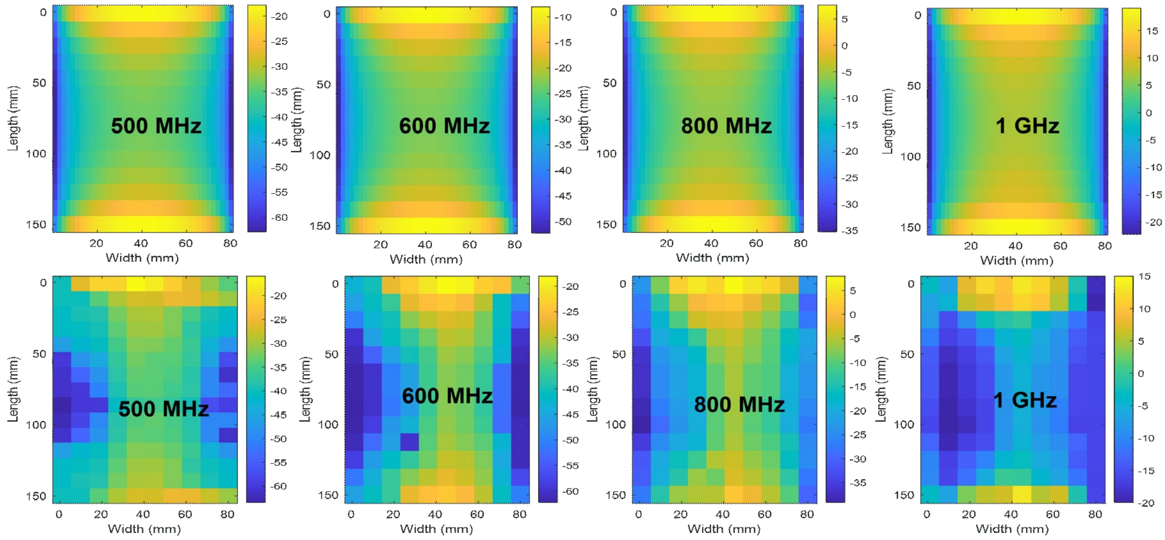


Fig. 5 Comparison of Simulated (1st row) vs. Measured (2nd row) $H_y$ $\sum |a_n|^2$ (dB).

The probe is moved over the entire area of the DUT with the help of the stepper motor. Fig. 4 compares the simulated and measured $H_x$ for four frequency points (500 MHz, 600 MHz, 800 MHz, and 1 GHz). The measurement and simulation results correlate well for all the frequency points with an error margin of 3.5 dB. Similarly, Fig. 5 compares the simulated and measured for Hy probe. Simulation and measurement results correlate well with an error of 4 dB for 500 MHz, 600, and 800 MHz. For 1 GHz, the error margin is 6.5 dB.

## V. Conclusion

This work proposes an experimental validation method for CMA using a reverberation chamber and near-field scanning system.

With the help of the modified MWC expression based on dipole sources, the TRP is obtained, which is compared with the measurement results obtained from the reverberation chamber. A good correlation between simulation and measurement with an error of 4 dB is achieved in the frequency range between 500 and 800 MHz.

## References

[1] M. Z. Hamdalla et al., "Characteristic Mode Analysis Prediction and Guidance of Electromagnetic Coupling Measurements to a UAV Model," *IEEE Access*, vol. 10, pp. 914-925, Jan 2022.

[2] X. Yang, Y. Liu and S. -X. Gong, "Design of a Wideband Omnidirectional Antenna With Characteristic Mode Analysis," *IEEE Antennas and Wireless Propag. Lett.*, vol. 17, no. 6, pp. 993-997, June 2018.

[3] H. Li, Y. Tan, B. K. Lau, Z. Ying and S. He, "Characteristic Mode Based Tradeoff Analysis of Antenna-Chassis Interactions for Multiple Antenna Terminals," *IEEE Trans. on Antennas and Propag.*, vol. 60, no. 2, pp. 490-502, Feb. 2012.

[4] F. H. Lin and Z. N. Chen, "Low-Profile Wideband Metasurface Antennas Using Characteristic Mode Analysis," *IEEE Trans. on Antennas and Propag.,* vol. 65, no. 4, pp. 1706-1713, April 2017.

[5] Y. S. Cao, Y. Wang, L. Jiang, A. E. Ruehli, J. Fan and J. L. Drewniak, "Quantifying EMI: A Methodology for Determining and Quantifying Radiation for Practical Design Guidelines," in *IEEE Trans. on Electromagnetic Compatibility*, vol. 59, no. 5, pp. 1424-1432, Oct. 2017

[6] X. Yang et al., "EMI Radiation Mitigation for Heatsinks Using Characteristic Mode Analysis," 2018 IEEE Symposium on Electromagnetic Compatibility, Signal Integrity and Power Integrity (EMC, SI & PI), Long Beach, CA, USA, 2018, pp. 374-378.

[7] X. Wang, D. Kim, C. Hwang, "On the Radio Frequency Interference Problem based on Characteristic Mode Analysis", submitted to *IEEE Transactions on Electromagnetic Compatibility.*

[8] F. A. Dicandia, S. Genovesi, and A. Monorchio, ''Efficient excitation of characteristic modes for radiation pattern control by using a novel balanced inductive coupling element,'' *IEEE Trans. Antennas Propag*., vol. 66, no. 3, pp. 1102–1113, Mar. 2018

[9] R. Harrington and J. Mautz, "Theory of characteristic modes for conducting bodies," *IEEE Trans. on Antennas and Propag.*, vol. 19, no. 5, pp. 622–628, 1971